ELSEVIER

Non-exponential relaxation of a single quantum vibrational excitation of a large molecule in collision free gas phase at elevated temperature

D.J. Myers [a], Motoyuki Shigeiwa [a], M.D. Fayer [a,*], Robert Silbey [b]

[a] *Department of Chemistry, Stanford University, Stanford, CA 94305, USA*
[b] *Department of Chemistry and Center for Materials Research, Massachusetts Institute of Technology, Cambridge, MA 02139, USA*

Abstract

The intramolecular vibrational dynamics of the asymmetric CO stretch of $W(CO)_6$ (~ 2000 cm^{-1}) have been studied in the collision free gas phase at 326 K using ps mid-infrared pump–probe spectroscopy. The pump–probe decay is a tri-exponential with components 140 ps, 1.28 ns, and > 100 ns. The middle component is the population relaxation into the collection of low frequency intramolecular modes. This relaxation heats the low frequency modes causing a spectral shift that gives rise to the long component. The fast component, which is described theoretically, is caused by the dynamics of the superposition state composed of thermally populated low frequency modes. © 1999 Elsevier Science B.V. All rights reserved.

1. Introduction

In this Letter, experiments and theory are presented to describe intramolecular vibrational dynamics following IR excitation of one quantum of the asymmetric CO stretching mode (~ 1990 cm^{-1}) of $W(CO)_6$ in the collisionless gas phase at 326 K. $W(CO)_6$ is a moderately sized molecule that has a large number of low frequency vibrational modes. It is small enough that the modes can be readily enumerated, but, because it has a significant number of low frequency modes, it is prototypical of large molecules. The vibrational lifetime, T_1, of the asymmetric CO stretch of $W(CO)_6$ has been measured in

a number of liquids [1,2] and as a function of density in several supercritical fluids [3], permitting comparison of the vibrational dynamics in dense media with dynamics in the gas phase.

There exists a vast amount of theory and experimental work on the vibrational states and vibrational dynamics of molecules. A great deal of work has focussed on small molecules, e.g., acetylene [4,5] and CO_2 [6]. Such molecules are frequently studied with very high spectral resolution at low temperatures (supersonic molecular beams). The experiments examine the vibrational spectra to very high energy with an eye to obtaining a detailed understanding of the vibrational eigenstates [7]. Vibrational relaxation has been studied in large molecules in both the frequency [8–10] and time domains [10–12] using electronic excitation. For example, vibronic excita-

---

* Corresponding author. Fax: +1-650-723-4817; e-mail: fayer@fayerlab.stanford.edu

tion and fluorescence detection were used to study alkyl substituted cold benzene, and dynamics were deduced from the line shapes [8,9]. Increased linewidths, which can reflect the vibrational lifetime, are observed as the size of the substituent is increased. The decrease in the vibrational lifetime arises from the increased density of vibrational states. Time domain experiments commonly involve electronic excitation followed by crossing into a very highly excited vibrational state of the ground electronic state [11].

In the experiments discussed below, a single quantum $(0 \to 1)$ of a high frequency vibrational mode is excited directly with an infrared (IR) pump pulse, and the time evolution of the system is followed with a variable time delayed IR probe pulse. The ensemble of molecules is in thermal equilibrium at a relatively high temperature. Thus, prior to IR excitation, the molecules have thermally populated low frequency modes, which contain considerable vibrational energy. A number of questions present themselves. For a molecule that is large enough to have low frequency modes and hot enough for those modes to be thermally populated, what is the nature of the vibrational dynamics in the absence of collisions? What is the relationship between the collision free dynamics and the dynamics in dense matter, e.g., liquids or supercritical fluids?

The results of the IR pump–probe experiments presented below are surprising. The observed decay of the asymmetric CO stretch is a tri-exponential with components of 140 ps, 1.28 ns, and > 100 ns. The middle component is identified as T_1, the time for population to flow out of the CO stretch. The slow component is caused by the deposition of ~ 2000 cm^{-1} of energy (T_1 process) into the low frequency modes, heating them substantially, which produces a frequency shift of the spectrum, preventing recovery of the ground state absorption. We suggest that the fastest decay component is caused by coupling of the thermally populated low frequency modes to the transition probability of the high frequency CO stretch. Addition of Ar to the sample cell causes the slowest and fastest components of the decay to become shorter as the Ar pressure is increased. At sufficiently high Ar pressure, the decay becomes single exponential, but T_1 is unchanged.

2. Experimental procedures

The experimental set-up has been discussed in detail previously [3,13]. The outputs of a doubled, mode-locked and Q-switched Nd:YAG laser and a tunable sync pumped dye laser are used to pump an optical parametric amplifier (OPA). The output of the OPA is a 1.5 μJ, 40 ps pulse at ~ 5 μm. The pulse has a bandwidth of 0.8 cm^{-1}. The IR pulse is beam split to form the pump and probe pulses. The probe pulse is passed down a 12 ns variable delay line.

A small amount of solid W(CO)$_6$ was placed in an evacuated 1.5 cm long stainless steel cell with CaF$_2$ windows. The pressure in the sample cell is the vapor pressure of W(CO)$_6$. The cell was heated to 326 K to increase the vapor pressure, producing an optical density 0.5–1.0. The frequency of the dye laser was tuned so that the infrared frequency was at the peak of the T_{1u} asymmetric CO stretch at 1997 cm^{-1}. Typical pump energies were ~ 700 nJ.

3. Results and discussion

Fig. 1 shows a typical $$FT-IR spectrum of gas phase W(CO)$_6$ in the 2000 cm^{-1} region. Spectra were taken directly in the cell by bringing the FT-IR beam out of the spectrometer, through the sample cell, and into a remote detector. Note that the P-, Q-, and R-branches are visible. Individual J states cannot be resolved because the rotational constant is very small (0.02 cm^{-1}). The IR pulse spectrum (FWHM of 0.8 cm^{-1}) is also shown. Note that the IR pulse spectrum is substantially narrower than the absorption spectrum. Experiments described here were performed at the center of the Q-branch. A subsequent publication will discuss measurements on the R- and P-branches [14].

Fig. 2 displays data taken at 326 K on the gas phase sample. The data are clearly non-exponential. The data can be fit very well with a tri-exponential. The average values are 140 ± 25 ps, 1.28 ± 0.09 ns, and > 100 ns. These values are substantially different, permitting the three components to be reliably separated. The slowest component is too slow to obtain an accurate measurement of the decay time, but it is clearly very long. All pump–probe measured
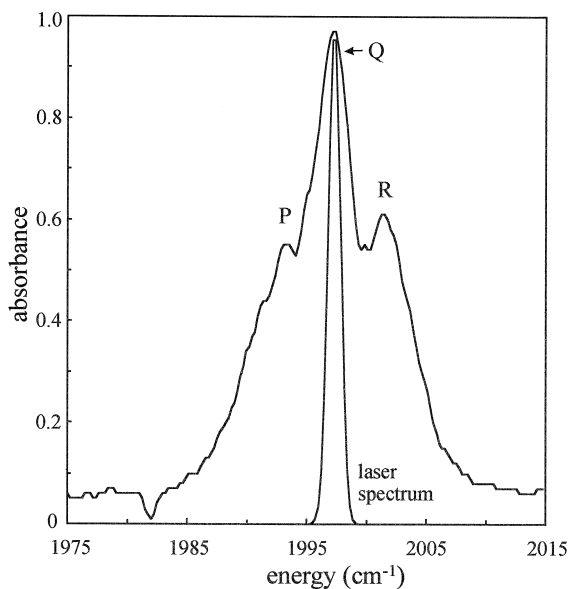
Fig. 1. FT-IR spectrum of $W(CO)_6$ in the gas phase at 326 K. The P-, Q-, and R-branches of the ν_6 vibration (CO asymmetric stretch, T_{1u}) are labeled. The rotational constant B is quite small (0.02 cm^{-1}) so the individual J lines are not resolved. Also shown is the spectrum of the infrared laser pulse, FWHM 0.8 cm^{-1}.

ture, no signal can be detected, showing that the pump–probe signal is due solely to gaseous $W(CO)_6$, and not $W(CO)_6$ crystallized on the window surfaces. Experiments with the probe at the magic angle and a variety of other angles show no change either in the decay times or the amplitudes of the components. Therefore, orientational dynamics are not contributing to the decays. (Orientational dynamics should occur on a time scale much faster than that of the experiments.) The only significant gas in the cell is $W(CO)_6$ itself. $W(CO)_6$ is at very low concentration (10^{-5} mol/l), which suggests a hard sphere time between collisions of 10^{-6} s. The possibility of very long range interactions was tested. By varying the temperature a few degrees, the $W(CO)_6$ concentration (vapor pressure) can be varied by over an order of magnitude. The change in concentration did not affect the tri-exponential decay.

The explanation for the slowest component in the tri-exponential decay is relatively straightforward. All of the modes of $W(CO)_6$ are known. Using the frequencies of the $W(CO)_6$ modes the average total

lifetime decays of $W(CO)_6$ in three supercritical solvents, ethane, CO_2 and fluoroform, over a wide range of densities (> 1 mol/l) and temperatures, are single exponentials [3,15,16]. In addition, measurements in liquids, such as CCl_4, at the magic angle, which eliminates orientational relaxation, also give single exponential pump–probe decays [1].

Fig. 3 shows the extrapolation of six density dependent sets of single exponential population decay rate constants ($W(CO)_6$ in three supercritical solvents, ethane, CO_2, and fluoroform, at two temperatures) to zero density. The spread in the extrapolations comes from making a linear extrapolation using only the lowest density data, which have the largest error bars. From the extrapolations, the zero density lifetime is ~ 1.1 ns. Therefore, we identify the middle component of the observed tri-exponential gas phase decay as the population relaxation lifetime, $T_1 = 1.28$ ns.

To explain the other two components, a number of experiments were conducted to rule out various possibilities. Careful intensity studies showed no power effects. When the sample is at room tempera-

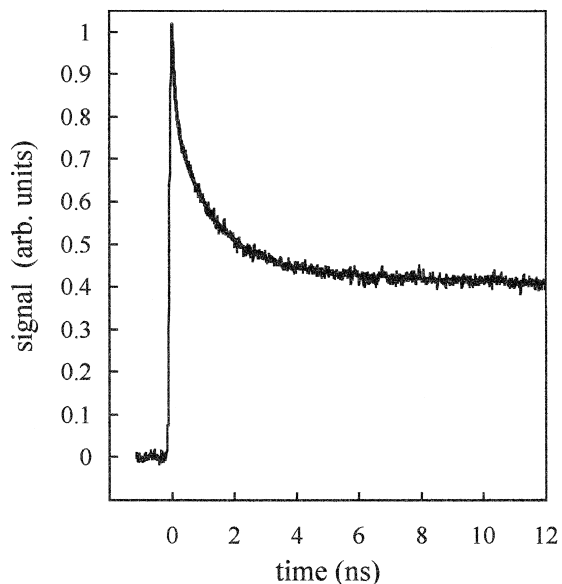
Fig. 2. Typical pump–probe data for the CO asymmetric stretch of $W(CO)_6$ in the gas phase at 326 K. The fit (barely discernable) is a tri-exponential with components 113 ps, 1.26 ns, and 157 ns. The values reported in the text are averages of many different data sets taken on many samples.
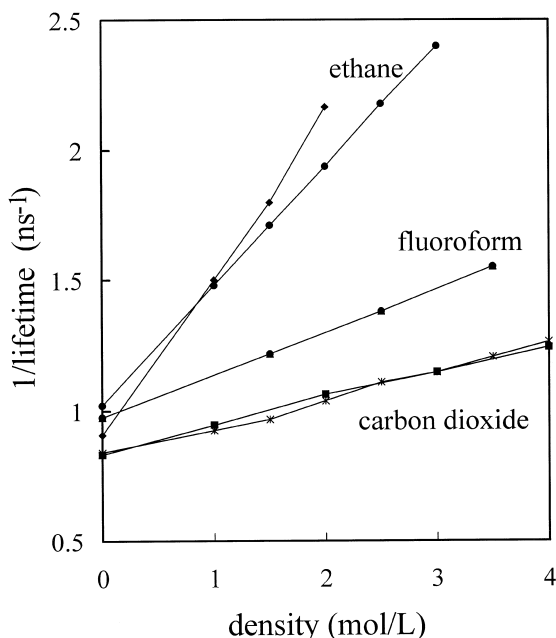
Fig. 3. Vibrational relaxation rate data for the CO asymmetric stretch of $W(CO)_6$ in various supercritical fluids at low densities. Extrapolation of the data to zero density gives an estimate of the gas phase (collisionless) lifetime of ~ 1.1 ns.

internal vibrational energy (all modes) was determined. For $T = 326$ K, the average energy is 2900 cm^{-1}. When the high frequency CO stretch relaxes, 2000 cm^{-1} of additional energy is deposited into the low frequency modes. Because the molecules are collision free on the time scale of the experiments, the extra 2000 cm^{-1} cannot leave the molecule. The deposition of energy raises the vibrational temperature for the average molecule to 450 K. Fig. 4 shows the measured temperature dependence of the Q-branch peak position as a function of temperature. The figure shows that as the temperature is increased, the spectrum red shifts.

Following a pump pulse that produces vibrational excitations, the probe pulse transmission through the sample is increased. A pump–probe signal has two contributions, stimulated emission and ground state depletion. These two contributions are equal; each contribution is 50% of the signal. As the excited state population relaxes into a combination of low frequency modes, the stimulated emission is reduced. Normally, it is expected that relaxation of the excited state population fills in the ground state depletion.

Thus, the stimulated emission and the ground state depletion decay together.

However, in the system under study here, relaxation of the 2000 cm^{-1} CO stretch into a combination of low frequency modes heats the molecules substantially and shifts the absorption spectrum to the red. First, consider the case in which the absorption shift is very large. Although the CO stretch is no longer excited, the ground state absorption is not recovered because the molecules that have undergone excitation and relaxation do not absorb at their initial frequency. Thus, the stimulated emission contribution to the signal is lost, but the ground state depletion at the probe frequency still exists. The signal will decay to 50%, and, in the absence of other processes, the signal will remain at 50%. Examining Fig. 2, it is seen that the slow component of the decay is somewhat below 50%. The decay to a value of less than 50% occurs because the spectral shift is relatively small when the molecule is heated by relaxation to ~ 450 K. The shift is ~ 1.1 cm^{-1},
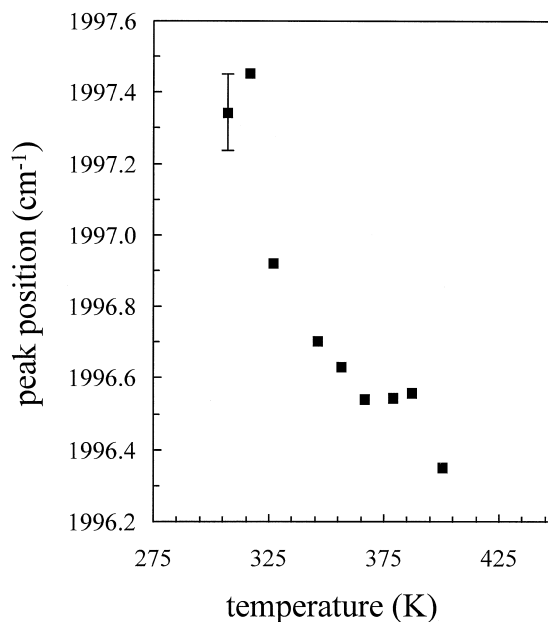

Fig. 4. Absorption frequency (Q-branch) versus temperature for the CO asymmetric stretch of $W(CO)_6$ in the gas phase. A representative error bar is shown. Extrapolation to 450 K (internal vibrational temperature following relaxation of the 2000 cm^{-1} CO stretch) yields a temperature dependent shift of ~ 1.1 cm^{-1} from the peak position at 326 K, the initial sample temperature.

which does not completely shift the relaxed population off of the probe absorption. Thus the ground state depletion within the probe bandwidth recovers to some extent, and the signal decays to less than 50%. The signal will eventually recover as infrequent collisions cool the molecules and cold molecules from other parts of the cell move into the probe volume. We estimate that the time scale for these processes is approximately the same, i.e., ~ 1 μs. Thus, over the 12 ns of delay used in the experiments, the long component appears essentially flat.

Fig. 5a shows a decay curve with a moderate pressure (0.05 mol/l) of Ar in the cell. The slow decay component is now noticeably faster, with a decay time of 8.1 ns. Collisions with Ar cool the low frequency modes, allowing the spectrum to return to its initial wavelength, which results in ground state recovery. Fig. 5b shows data with an even higher Ar pressure. The decay is now a single exponential. The collision induced cooling is fast compared to T_1, and the stimulated emission and ground state depletion decay together, eliminating the long lived component. It is interesting to note that while Ar is effective in causing the energy in the low frequency modes to relax into the bath, the value of T_1 remains unchanged. This is in contrast to experiments in polyatomic solvents, such as ethane, where T_1 becomes shorter as the solvent density is increased. Detailed analysis of the long component, including measurements on the P- and R-branches, will be presented in a subsequent publication [14].

We propose that the fast component of the tri-exponential decay (140 ps) can be explained by the influence of the low frequency modes of the molecule on the high frequency CO stretch. In the gas phase vibrational experiment, prior to application of the pump pulse, the initial state of the molecule is prepared by its last collision with the wall of the cell or another molecule. The initial state is a complex superposition of eigenstates. Each mode, λ, will have some occupation number, n_λ. Under collision free conditions, for a given molecule, the n_λ are fixed. At the 326 K sample temperature, the average total internal vibrational energy of a molecule is 2900 cm^{-1}, and the density of states at this energy (calculated with the harmonic approximation) is 5×10^5 states/cm^{-1} [17,18]. Thus, there are a vast
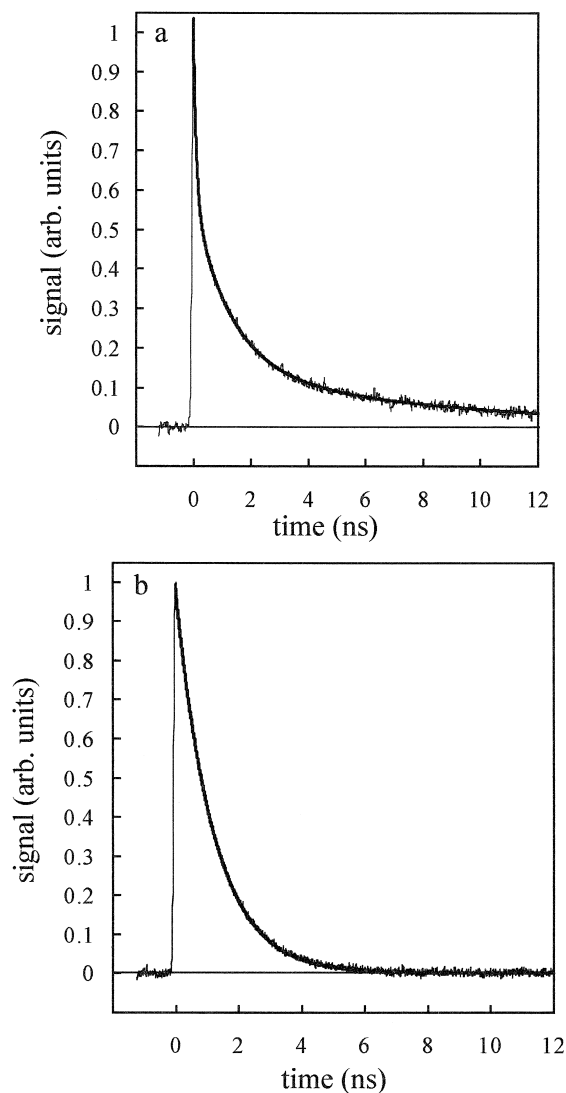

Fig. 5. Sample pump–probe scans on the CO asymmetric stretch of W(CO)$_6$ in argon at two different pressures at 333 K (60°C). (a) Pressure = 18 psia (~ 1 atm). Argon density of ~ 0.05 mol/l and inverse collision frequency of ~ 0.2 ns. The decay is fitted with tri-exponential components 107 ps, 1.29 ns and 8.1 ns. The long component has become substantially faster compared to collision free conditions. Argon permits vibrational cooling of the vibrationally excited W(CO)$_6$ molecules through collisions. The cooling eliminates the spectral shift, which is responsible for the long decay component, and the decay becomes faster. (b) Pressure = 1100 psia. Argon density of ~ 3 mol/l. The decay is now a single exponential with lifetime 1.20 ns. The fastest and slowest tri-exponential components observed in the gas phase (Fig. 2) are eliminated by rapid collisions with argon at this high pressure (inverse collision frequency of ~ 3 ps). The lifetime is unchanged from the gas phase value, within experimental error.

number of initial states of the molecules that comprise the experimental ensemble. Absorbing a photon, which takes a molecule from the 0 to 1 state of the high frequency CO stretch, changes the potential of the low frequency modes. The change in potential produces a time evolution that influences the CO stretch optical transition probability measured by the probe pulse.

As a first approach to describing the fast time evolution of the system quantitatively, a description using a harmonic basis set with anharmonic coupling of the high frequency CO stretch and the other modes can be employed. The Hamiltonian for the system is

$$H = \sum_\lambda \left(\tfrac{1}{2} P_\lambda^2 + \tfrac{1}{2} \omega_\lambda^2 q_\lambda^2 \right) + \left(\tfrac{1}{2} P^2 + \tfrac{1}{2} \Omega^2 Q^2 \right)$$
$$+ V(Q, \{q_\lambda\}), \qquad (1)$$

where the sum is over the harmonic part of all modes, q_λ, other than the high frequency asymmetric CO stretching mode, the second term in brackets is for the CO stretching mode, Q, and the last term is the potential for the anharmonic interactions among modes. Since the experiments only involve the ground and first excited vibrational states of the CO stretch, the Hamiltonian can be restricted to that space. Then,

$$H = \sum_\lambda \left(\tfrac{1}{2} P_\lambda^2 + \tfrac{1}{2} \omega_\lambda^2 q_\lambda^2 \right) + E_0 |0\rangle\langle 0|$$
$$+ (E_0 + \Omega)|1\rangle\langle 1|$$
$$+ V_0 |0\rangle\langle 0| + V_1 |1\rangle\langle 1|, \qquad (2)$$

where

$$V_0 = \langle 0|V(Q, \{q_\lambda\})|0\rangle \equiv V_0(\{q_\lambda\}), \qquad (3)$$
$$V_1 = \langle 1|V(Q, \{q_\lambda\})|1\rangle \equiv V_1(\{q_\lambda\}). \qquad (4)$$

V_0 is the anharmonic interaction when the CO stretch is in the ground vibrational state, and V_1 is the anharmonic interaction when the CO stretch is in its first excited vibrational state. To simplify the analysis, take $E_0 = 0$, and transform into the interaction representation with respect to all of the $\{q_\lambda\}$. Further, take $V_0 = 0$, which restricts the analysis to the excited vibrational state but does not fundamentally change the nature of the results. Then, the effective Hamiltonian for the CO stretch is

$$H_{\text{eff}}(t) = \Omega|1\rangle\langle 1| + V_1(\{q_\lambda(t)\})|1\rangle\langle 1|. \qquad (5)$$

Initially the CO stretch is in the ground state, so $\psi = |0\rangle$. The laser prepares the state $|1\rangle$, and the system evolves as

$$|\psi(t)\rangle = U(t)|1\rangle = e^{-i\Omega t} e_o^{-i\int_0^t V_1(q_\lambda(\tau))d\tau} |1\rangle, \qquad (6)$$

where $U(t)$ is the propagator, and e_o is the time ordered exponential. For a pump–probe experiment, we need the probability, $P(t)$, of making a transition back to $|0\rangle$. $P(t)$ depends on the dynamics of the low frequency modes and is obtained through an average over the initial states of $\{q_\lambda\}$.

$$P(t) \propto \overline{|\langle 0|\mu|\psi(t)\rangle|^2} \propto \overline{|\langle 1|\psi(t)\rangle|^2}, \qquad (7)$$

where μ is the transition dipole operator, and the bar over the expression indicates the aforementioned average. Substituting Eq. (6) for Eq. (7) gives

$$P(t) = A \left| \overline{\langle 1| e^{-i\int_0^t V_1(q_\lambda(\tau))d\tau} |1\rangle} \right|^2, \qquad (8)$$

with A being a constant. As an initial approximation, the average in Eq. (8) can be replaced by a second cumulant approximation, i.e.,

$$\overline{\exp\left(-i\int_0^t V_1(\tau)d\tau \right)}$$
$$\cong \exp\left(-\int_0^t d\tau_2 \int_0^{\tau_2} d\tau_1 \overline{V_1(\tau_2)V_1(\tau_1)} \right). \qquad (9)$$

Using Eq. (9) in Eq. (8) and accounting for the absolute value squared,

$$P(t) = \langle 1| \exp\left(-2\text{Re} \int_0^t d\tau_2 \right.$$
$$\left. \times \int_0^{\tau_2} d\tau_1 \langle V_1(\tau_2)V_1(\tau_1)\rangle \right) |1\rangle, \qquad (10)$$

where Re indicates the real part of the expression and $\langle\ \rangle$ is now used to indicate the average.

To evaluate Eq. (10), we consider a simple model in which the potential V_1 depends on the coupling between modes as,

$$V_1(\{q_\lambda\}) = \sum_{\lambda\mu'} c_{\lambda\mu} q_\lambda q_\mu, \qquad (11)$$

where $c_{\lambda\mu}$ is the coupling constant and $\lambda \neq \mu$. The q can be written in terms of raising and lowering operators, b_λ^+ and b_λ, respectively. Then

$$V_1(\{q_\lambda(\tau)\}) = \sum_{\lambda\mu} c'_{\lambda\mu} \left[b_\lambda e^{-i\omega_\lambda\tau} + b_\lambda^+ e^{i\omega_\lambda\tau} \right]$$

$$\times \left[b_\mu e^{-i\omega_\mu\tau} + b_\mu^+ e^{i\omega_\mu\tau} \right]. \qquad (12)$$

Using this expression for V_1, the correlation function in the exponent of Eq. (10) becomes,

$$\text{Re}\langle V_1(\tau_2) V_1(\tau_1) \rangle$$

$$= \text{Re} \sum_{\lambda,\mu} |c'_{\lambda\mu}|^2 \Big[(n_\lambda + 1) e^{-i\omega_\lambda(\tau_2-\tau_1)}$$

$$+ n_\lambda e^{i\omega_\lambda(\tau_2-\tau_1)} \Big] \Big[(n_\mu + 1) e^{-i\omega_\mu(\tau_2-\tau_1)}$$

$$+ n_\mu e^{i\omega_\mu(\tau_2-\tau_1)} \Big]. \qquad (13)$$

Substituting Eq. (13) into Eq. (10) and performing the integrals gives a final result

$$P(t) = A \exp\Bigg[-2 \sum_{\lambda,\mu} |c'_{\lambda,\mu}|^2$$

$$\times \Bigg\{ \big[n_\lambda n_\mu + (n_\lambda + 1)(n_\mu + 1) \big]$$

$$\times \left(\frac{1 - \cos[(\omega_\lambda + \omega_\mu)t]}{(\omega_\lambda + \omega_\mu)^2} \right)$$

$$+ \big[n_\lambda(n_\mu + 1) + n_\mu(n_\lambda + 1) \big]$$

$$\times \left(\frac{1 - \cos[(\omega_\lambda - \omega_\mu)t]}{(\omega_\lambda - \omega_\mu)^2} \right) \Bigg\} \Bigg]. \qquad (14)$$

Even for the simple model of cubic anharmonic coupling ($Qq_\lambda q_\mu$) of the high frequency mode Q and the low frequency modes $\{q_\lambda\}$, Eq. (14) demonstrates that the pump–probe signal will have a time dependence in addition to the vibrational lifetime, T_1. (Note that for $W(CO)_6$, $\omega_\lambda = \omega_\mu$ will not appear in the sum since the coupling coefficient for such terms will vanish. Q is an antisymmetric mode. For $\omega_\lambda = \omega_\mu$, the modes q_λ and q_μ are members of a degenerate mode. Therefore, the direct product of their irreducible representations is symmetric, and the matrix element vanishes by symmetry.) Eq. (14) describes the time dependence of a single molecule. The time dependence depends on the frequencies of the low frequency harmonic modes, the coupling strengths of the modes, and the occupation numbers of the modes. While the harmonic mode frequencies and the coupling strengths will be identical for all molecules, the occupation numbers will differ. Each molecule will display a complex time dependence. $W(CO)_6$ has 27 low frequency modes, ranging in frequency from 60 to 590 cm^{-1}. Thus the time dependence will be complicated, and in principle, recurrences are possible. However, the values of the occupation numbers, n_i, will vary widely from one molecule to the next. It is anticipated that the ensemble average over the various combinations of occupation numbers will eliminate the oscillatory nature of the time dependence and lead to a monotonic decay.

As shown in Fig. 5b and in many other experiments [1,3,15,16], the decay of the CO stretch is a single exponential when $W(CO)_6$ has substantial interactions with a solvent. A single exponential (aside from orientational relaxation in liquids) is observed even when very fast pulses are used in the experiments [19]. In the gas phase, the transition frequency of the CO stretch evolves over a range of frequencies because of its time dependent interaction with the low frequency modes. When a buffer gas or solvent is added, collisions cause the coherent evolution of the slow modes to be interrupted frequently, resulting in a narrowing of the CO asymmetric stretch 0–1 transition and *possibly* an averaging away of the perturbation responsible for the observed fast time dependence. Thus, the fast component observed in these experiments is inherently a low pressure, gas phase phenomenon.

References

[1] A. Tokmakoff, B. Sauter, M.D. Fayer, J. Chem. Phys. 100 (1994) 9035.

[2] E.J. Heilweil, R.R. Cavanagh, J.C. Stephenson, Chem. Phys. Lett. 134 (1987) 181.

[3] R.S. Urdahl, D.J. Myers, K.D. Rector, P.H. Davis, B.J. Cherayil, M.D. Fayer, J. Chem. Phys. 107 (1997) 3747.

[4] S.A.B. Solina, J.P. O'Brien, R.W. Field, W.F. Polik, Ber. Bunsenges. Phys. Chem. 99 (1995) 555.

[5] D.M. Jonas, S.A.B. Solina, B. Rajaram, R.J. Silbey, R.W. Field, J. Chem. Phys. 97 (1992) 2813.

[6] M.S. Elioff, M.C. Wall, A.S. Lemoff, A.S. Mullin, J. Chem. Phys. 110 (1999) 5578.

[7] K.K. Lehmann, G. Scoles, B.H. Pate, Annu. Rev. Phys. Chem. 45 (1994) 241.

[8] J.B. Hopkins, D.E. Powers, R.E. Smalley, J. Chem. Phys. 72 (1980) 5039.

[9] J.B. Hopkins, D.E. Powers, S. Mukamel, R.E. Smalley, J. Chem. Phys. 72 (1980) 5049.

[10] A.S. Mullin, G.C. Schatz (Eds.), Highly Excited Molecules, ACS Symposium Series, Vol. 678, American Chemical Society, Washington, DC, 1997.

[11] D. Schwarzer, J. Troe, M. Votsmeier, M. Zerezke, J. Chem. Phys. 105 (1996) 3121.

[12] B. Abel, N. Lange, F. Reiche, J. Troe, J. Chem. Phys. 110 (1999) 1404.

[13] A. Tokmakoff, C.D. Marshall, M.D. Fayer, JOSA B 10 (1993) 1785.

[14] D.J. Myers, M. Shigeiwa, R. Silbey, M.D. Fayer, submitted for publication.

[15] D.J. Myers, S. Chen, M. Shigeiwa, B.J. Cherayil, M.D. Fayer, J. Chem. Phys. 109 (1998) 5971.

[16] D.J. Myers, R.S. Urdahl, B.J. Cherayil, M.D. Fayer, J. Chem. Phys. 107 (1997) 9741.

[17] L.H. Jones, R.S. McDowell, M. Goldblatt, Inorg. Chem. 8 (1969) 2349.

[18] D.C. Astholz, J. Troe, W. Wieters, J. Chem. Phys. 70 (1979) 5107.

[19] A. Tokmakoff, R.S. Urdahl, D. Zimdars, R.S. Francis, A.S. Kwok, M.D. Fayer, J. Chem. Phys. 102 (1995) 3919.